Conformational Preferences of Linear β-Defensins Are Revealed by Ion Mobility-Mass Spectrometry

Martin De Cecco,[†] Emily S. Seo,[†] David J. Clarke,[†] Bryan J. McCullough,[†,⊥] Karen Taylor,[‡] Derek Macmillan,[§] Julia R. Dorin,[‡] Dominic J. Campopiano,[†] and Perdita E. Barran*[,†]

School of Chemistry, University of Edinburgh, Edinburgh, EH9 3JJ, U.K., Medical Research Council Human Genetics Unit, Edinburgh, EH4 2XU, U.K., Department of Chemistry, Christopher Ingold Laboratories, University College London, London, WC1H 0AJ, U.K.

Received: November 24, 2009; Revised Manuscript Received: January 11, 2010

In recent times there has been an enormous rise in resistance to synthetic antibiotics as well as an increase in the virulence of bacteria, the so-called "superbugs". This problem has catalyzed a search for novel molecules to fight bacteria, which in turn relies on a better understanding of the molecular basis of the immune response. β-defensins are a class of small, cationic, cysteine-rich antimicrobial peptides expressed by humans and other animals to act against incoming pathogens. As well as their antimicrobial properties, β-defensins also act as chemokines, recruiting cells to the sites of infection. Here the relationship between the tertiary structures of β-defensin analogs and their chemotactic activities has been investigated using ion mobility-mass spectrometry (IM-MS) and biochemical assays. A panel of derivatives of the murine β-defensin Defb14 has been formed and the ability of these peptides to chemoattract the receptor CCR6 has been assessed in vitro. The derivatives can be divided into two groups, those with chemotactic activity equal to that of the unmodified parent peptide, and those whose chemotactic activity has been lost upon modification. Analysis by ion mobility-mass spectrometry reveals the conformational preferences of these peptides upon ionization from different solvents. Under denaturing conditions, the chemotactic peptides adopt more compact conformations in the gas-phase at higher charge states than those which are inactive. While the conditions of these experiments are not akin to the environment around the receptor in vivo, this technique provides an in vacuo method for distinguishing between the different chemotactic activities of β-defensin derivatives.

Introduction

We are exposed to thousands of pathogenic organisms on a daily basis yet humans succumb to infection relatively rarely. We are mostly able to survive this onslaught due to a sophisticated defense mechanism, the immune response, which can detect and kill numerous pathogens even though they are constantly evolving under selective pressure to escape destruction by their human hosts. However, the rapid increase in mammalian resistance to common antibiotics and the parallel rise of "superbugs" has catalyzed a search for a more adaptable answer to controlling the spread of infections. The family of antimicrobial peptides known as defensins forms a critical part of the immune response of plants and animals to defeat incoming pathogens,[1–3] and hence form an ideal target of study to further our understanding of the molecular basis of antimicrobial resistance.

Defensins exhibit broad-spectrum antimicrobial activity toward a wide range of Gram-positive and Gram-negative bacteria. Interestingly, in addition to their ability to kill bacteria directly, defensins can also recruit host immune cells to fight infection. This occurs via the process of chemotaxis, whereby cells are attracted toward sites of increased concentration of defensins. First reported by De Yang et al. in 1999, human β-defensins were found to be selectively chemotactic for cells transfected to express the human chemokine receptor CCR6.[4] This raises the possibility of using defensin-inspired peptides as therapeutic agents to modulate the immune response.[5] Understanding the molecular basis of the defensin-receptor interaction would advance the development of drugs that mimic this important biological function and thus provide an alternative strategy to overcome bacterial infection.

β-defensins contain a highly conserved motif of six cysteines that oxidize to form three intramolecular disulfide bonds in a characteristic pattern ($C^{I}-C^{V}$, $C^{II}-C^{IV}$, $C^{III}-C^{VI}$). This is thought to be crucial in generating a conserved three-dimensional fold consisting of three antiparallel β-strands alongside an N-terminal α-helix region. It has been demonstrated that these disulfide bridges are not essential to the antimicrobial activity of β-defensins in vitro,[6,7] although they are thought to prevent proteolysis in vivo.[8] Meanwhile, the ability of human β-defensin 3 (HBD3) to induce chemotaxis was found to be highly dependent on the connectivities of the disulfide bonds.[6] Lu and collaborators observed that the chemotactic activities of six different topological analogs of HBD3 varied by 3−4 orders of magnitude. A linear, cysteine-free peptide was inactive.

Recently we have shown that variants of HBD3 and its mouse ortholog Defb14 that each have only one cysteine, at the fifth position (Cys^{V}), possess chemotactic properties equivalent to those of their parent peptides.[7] The location of this cysteine residue is important; a peptide with a single cysteine in the first position (Cys^{I}) was found to be inactive against the CCR6 receptor. In agreement with the work of Lu and colleagues, we also observed that cysteine-free derivatives of HBD3 and Defb14

* To whom correspondence should be addressed. E-mail: Perdita.Barran@ed.ac.uk.
† University of Edinburgh.
‡ Medical Research Council Human Genetics Unit.
§ University College London.
⊥ Present address: LGC, Teddington, Middlesex, TW11 0LY, U.K.

10.1021/jp9111662
Published on Web 01/26/2010

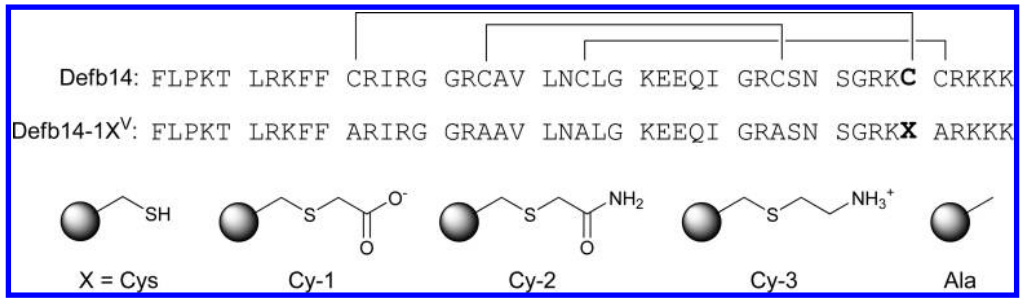

Figure 1. Sequences of Defb14 and its linear analogs, Defb14-1X^V. X = Cys represents the unmodified single-cysteine peptide. Cy-1 denotes the carboxymethylated derivative, Cy-2 the carboxamidomethylated derivative, and Cy-3 the ethylamine derivative. X = Ala indicates the substitution of every cysteine for alanine and is referred to as Defb14-0Cys in the text. The canonical β-defensin pattern of disulfide bridging is shown for Defb14.

do not chemoattract. Röhrl et al. demonstrated that a fusion protein, consisting of an immunoglobulin attached to the C-terminus of Defb14, was an active chemoattractant.[9] In another study, mutations of the N-terminal sequence of human β-defensin 1 were found to significantly decrease the peptide's affinity for the receptor.[10] Thus it appears that the relationship between primary structure, disulfide bridging, and biological activity is finely balanced within this important class of peptides and further analysis is required to tease out specific structure−function relationships.

Ion mobility-mass spectrometry (IM-MS) is emerging as a new tool for structural biology and medicine.[11−13] Ion mobility instrumentation determines the time it takes ions to pass through a drift cell containing an inert gas under the influence of a weak electric field.[14] The mobility of an ion is the constant of proportionality between the velocity at which it moves through the cell and the applied electric field and is inversely proportional to the collision cross-section (Ω) of the gas-phase ion according to the equation below

$$K_0 = \frac{3ze}{16N}\left(\frac{2\pi}{\mu k_B T}\right)^{1/2}\frac{1}{\Omega} \quad (1)$$

where K_0 is the reduced mobility (the measured mobility corrected to 273.15 K and 760 Torr), z is the ion charge state, e is the elementary charge, N is the gas number density, μ is the reduced mass of the ion-neutral pair, k_B is the Boltzmann constant, and T is the gas temperature. More compact ions will traverse the drift cell faster than more extended ions of the same m/z and so the conformations of mass-selected ions can be probed. For biomolecules, calculation of the collision cross-section provides information on the tertiary structure of the ion in a solvent-free environment.

In the mid-1990s, Bowers and co-workers used IM-MS to examine the conformational flexibility of peptide ions produced by matrix-assisted laser desorption ionization.[15] They discovered that protonated and sodiated monocations of bradykinin possess very similar cross sections, implying that the peptide adopts a globular fold that surrounds the point of charge. In addition, no significant change in cross-section was observed over the temperature range 300−600 K, signifying that this geometry is preferred even at higher temperatures. Early studies into the gas-phase conformations of peptide ions produced by electrospray ionization included the investigation of bovine pancreatic trypsin inhibitor (BPTI) by Clemmer, Jarrold, and colleagues.[16,17] They observed that the cross sections of BPTI ions did not vary with increased collisional energy. This reflects the stability of its three-dimensional structure, which is preserved by three intramolecular disulfide bonds. More recently, Schenauer and Leary applied IM-MS to the study of the monocyte chemotactic protein, MCP-1.[18] They found that the dimeric form of this polypeptide became more extended with increasing collisional activation. In contrast, the MCP-1 monomer formed by dissociation of the homodimer was as compact as the monomer found in solution. The authors attribute these findings to the dislocation of one monomer relative to the other during dissociation of the homodimer without any substantial unfolding of the monomeric subunits.

We have previously employed ion mobility to examine the conformations of β-defensins and related peptides with a particular emphasis on its use to reveal the conformational restriction imparted by disulfide bridges.[19,20] It is often difficult to assign the correct disulfide pairings in cysteine-rich peptides with confidence. For example, Defr1 Y5C contains 6 cysteine residues and has 15 possible connectivities. By combining ion mobility with molecular modeling, we were able to eliminate 10 of these different topologies on the basis of their cross-section. Here, we apply this technique to determine the collision cross sections of a panel of single-cysteine derivatives of Defb14 (Figure 1) and hence derive a correlation between peptide conformation and chemotactic activity. We also propose ion mobility mass spectrometry as a novel approach with which to determine the fold destabilization imparted by single point mutations in a protein sequence.

Methods

Peptide Synthesis. Defb14-1Cys^V was chemically synthesized and purified as described previously.[7] This was subsequently derivatized in-house as follows. All reagents were obtained from Sigma Aldrich.

Carboxymethylated Derivative, Defb14-1(Cy-1)^V. Two milligrams of Defb14-1Cys^V (0.40 μmol) was dissolved in Tris buffer, pH 7.5, and treated with 1 molar equivalence of tris(2-carboxyethyl)phosphine (TCEP) for 30 min. The solution was then treated with iodoacetate (10 equivalent, 4 μmol) and incubated at room temperature for 4 h. The reaction was quenched with dithiothreitol (DTT, 10 equivalent, 4 μmol) and purified by reverse-phase HPLC using a Jupiter Proteo column (Phenomenex).

Carboxyamidomethylated Derivative, Defb14-1(Cy-2)^V. Two milligrams of (0.40 μmol) Defb14-1Cys^V was dissolved in 1 mL of 0.1 M Tris buffer, pH 7.5, and treated with TCEP (1 equivalent, 0.40 μmol) as above. The solution was treated with iodoacetamide (5 equivalent, 2 μmol) and left to stir for 2 h in the dark or wrapped in tin foil. The reaction was then quenched with DTT (5 equivalent, 2 μmol) and purified as above.

Ethylamine Derivative, Defb14−1(Cy-3)^V. Five hundred micrograms of Defb14-1Cys^V (0.1 μmol) was dissolved in

degassed 2 mL of 0.1 M Tris buffer, pH 8.0 and treated with TCEP (1 equivalent, 0.1 μmol). An hour later, bromoethylamine hydrobromide (BEA, 10 equivalent, 1.0 μmol) was added and the reaction was incubated overnight under nitrogen in the dark. The next morning, additional BEA (10 equivalent, 1.0 μmol) was added, incubated overnight, and the reaction was purified the following day.

Chemotaxis Assays. The migration of HEK293 cells expressing CCR6 in response to peptides at different concentrations was assayed as described previously.[7] Three to five independent experiments were carried out, each of which was performed in triplicate.

Mass Spectrometry. Samples were prepared at a peptide concentration of 50 μM in either buffered (10 mM ammonium acetate) or denaturing (49.5% water, 49.5% methanol, 1.0% formic acid) solutions. Different solvent conditions were chosen to explore the conformational space available to each peptide as a function of their environment The peptide structure is expected to change to maximize favorable solute−solvent interactions, which are dependent on the pH and hydrophobicity of the solution.[21] Such changes in the conformation of a given peptide or protein in solution are reflected in a change in the charge state distribution in the mass spectrum[22] consistent with solvent memory being retained in the gas phase conformations. Mass spectra were recorded on a QToF II mass spectrometer (Waters, U.K.), using identical tuning conditions for each sample. Ions were produced by positive nanoelectrospray ionization with a capillary voltage of 1.6−2.0 kV and a source temperature of 80 °C. Nanoelectrospray tips were prepared in-house from borosilicate glass capillaries using a Flaming/Brown Micropipet puller. Voltage is applied to the spray solution via a platinum wire inserted into the capillary.

Ion Mobility-Mass Spectrometry. Samples for IM-MS were prepared and ionized by nanoelectrospray ionization as described above. Ion mobility measurements were made using a quadrupole time-of-flight mass spectrometer that had been modified in-house to include a 5.1 cm copper drift cell for ion mobility spectroscopy. The instrument has been described in detail previously,[20] but in brief ions produced in the Z-spray ion source are guided through a hexapole into the drift cell via an einzel lens. They pass through the drift cell where the buffer gas temperature and pressure are measured carefully (see below) and on exiting then pass via a short refocusing lens into a second hexapole and from that into a QToF I mass spectrometer (Waters, UK). In these experiments the quadrapole is used simply as a mass filter and the ions are mass analyzed by time-of-flight mass spectrometry. The signals from the ions arriving at the microchannel plate detector pass through a 4 GHz TDC card and are processed into mass spectra and arrival time distributions using MassLynx 4.1 (Waters, UK).

During each ion mobility separation, ions are accumulated in the precell region by raising the DC voltage on the lens element immediately prior to the entrance lenses of the drift cell. Using a pulse generator, the DC trapping voltage is then lowered for 40 μs to inject a pulse of ions into the drift cell. Ion arrival time distributions (mobility spectra) are recorded by synchronization of the release of ions into the drift cell with mass spectral acquisition. For each of the experiments in this study, the cell contained helium at a pressure of 3.0−3.5 Torr and a temperature of 37 ± 5 °C. The electric potential difference across the cell was varied from 60 to 15 V with measurements made at eight different voltages. A minimum of 10 mobility spectra were acquired at each drift voltage. Both pressure and temperature are recorded for every measurement taken. For each drift voltage, the pressure in the cell for that measurement does not drift by more than 0.01 Torr; for each experiment the temperature of the drift cell does not vary by more than 3 °C.

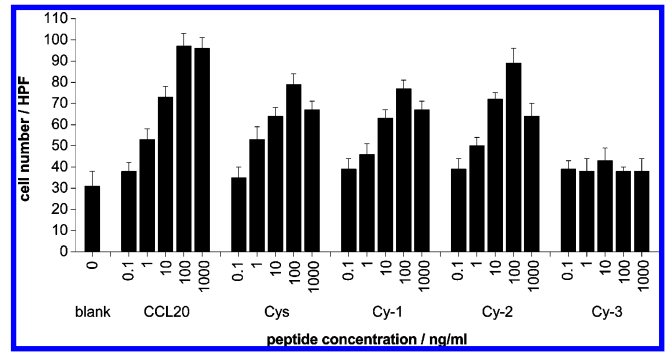

Figure 2. Chemotactic activity of the Defb14-1Cys^V derivatives. The migration of HEK293 cells expressing CCR6 in response to peptides at different concentrations was measured. Shown is the mean (±standard deviation) number of cells migrated per high power field (number/HPF). CCL20 is a known natural ligand for CCR6 and was used as a positive control. Blank refers to the medium alone.

Using the theory described above, the reduced mobility of each ion was calculated from the linear gradient of a plot of arrival time versus the ratio of pressure to drift voltage, for each of the eight voltages. Experimental data is fitted with a straight-line to a precision $R^2 \geq 0.999$. From this, the rotationally averaged collision cross-section of each analyte ion was determined. Analysis of each peptide was performed in triplicate and the mean collision-cross section was calculated.

Results and Discussion

Chemotaxis Assays. Our previous work showed that the cysteine residue at position V of Defb14 is essential for the chemotactic activity of this peptide.[7] It was surprising that changing cysteine to alanine, essentially the replacement of a thiol group with a hydrogen atom, had such a marked impact on the function of the 45 amino acid peptide. This raises the question: does the side-chain of this cysteine residue interact directly with CCR6, or is this cysteine residue important to the conformation of the rest of the molecule? This prompted us to synthesize a panel of derivatives of the single-cysteine containing peptide Defb14-1Cys^V and assess their chemotactic activity (Figure 2). The derivatives were chosen so that the panel contained peptides with a variety of different functional groups in the place of Cys^V.

Interestingly, the carboxymethylated (Defb14-1(Cy-1)^V) and the carboxamidomethylated (Defb14-1(Cy-2)^V) derivatives induce migration of significantly ($p < 0.05$) more cells than control medium alone, as was observed for unmodified Defb14-1Cys^V. In contrast, modification of Defb14-1Cys^V to form the ethylamine derivative (Defb14-1(Cy-3)^V) renders the peptide unable to induce cell migration, as seen for Defb14−0Cys.

Clearly, small chemical changes at a single residue of the Defb14-1Cys^V peptide greatly influence its ability to act as a chemoattractant. Given that Defb14-1(Cy-1)^V and Defb14-1(Cy-2)^V are as active as Defb14 and Defb14-1Cys^V despite the different functional groups of the side-chain at position V, it is unlikely that Cys^V interacts directly with CCR6. Our earlier work employed NMR spectroscopy and found that linear derivatives of Defb14 did not exhibit clear secondary structural elements in solution.[7] Analysis by circular dichroism spectroscopy (data not shown) shows each derivative in this study to be a mix of unstructured peptide and β-turn/strand in aqueous solution. Upon the addition of methanol, a more hydrophobic solvent, all of

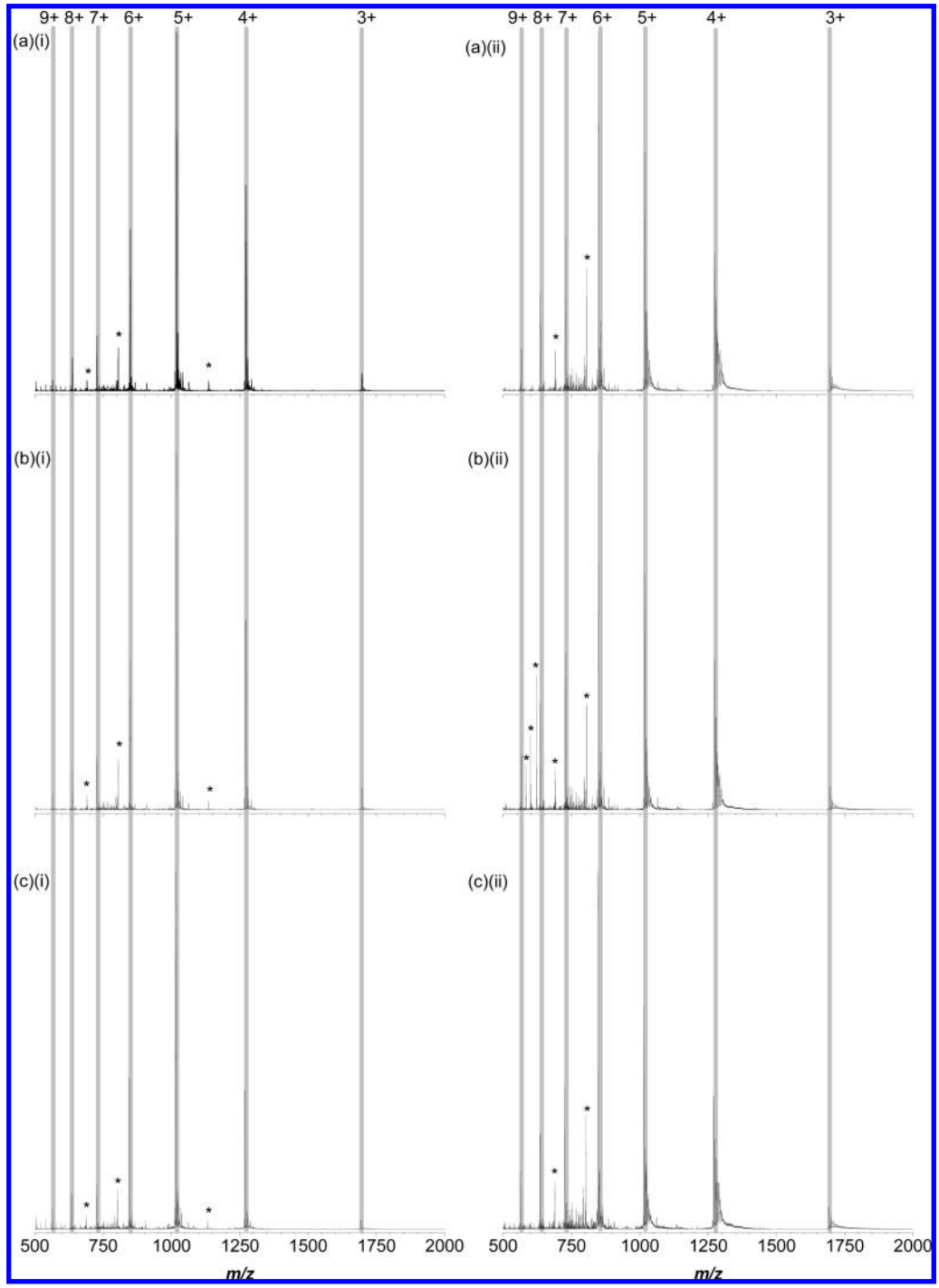

Figure 3. Mass spectra of the derivatives Defb14-1X^{V}. (a) Defb14-1(Cy-1)^{V}; (b) Defb14-1(Cy-2)^{V}; (c) Defb14-1(Cy-3)^{V}. Samples prepared at 50 μM in (i) 10 mM ammonium acetate; (ii) 49.5% water, 49.5% methanol, 1% formic acid. Charge states $[M + 3H]^{3+}$ to $[M + 9H]^{9+}$ are highlighted in gray. Peaks marked with an asterisk (*) correspond to impurities in the sample.

the linear peptides form an α-helix. Therefore the differences in chemotactic activity cannot be explained on the basis of any variation of the secondary structure of the free peptides in solution since no difference is observable. Instead, it is more likely that changing the chemistry of the thiol group has altered the conformational preference of the entire peptide, perhaps occurring only upon receptor binding.

Mass Spectrometry. The mass spectrum of each peptide displays several charge states corresponding to protonated species $[M + zH]^{z+}$ generated by nanoelectrospray ionization. In both ammonium acetate and acidified water/methanol, charge states $z = 3-9$ are observed for the derivatives of Defb14-1Cys^{V} (Figure 3). In comparison, $[M + 7H]^{7+}$ was the most highly charged species observed for the oxidized (six cysteine) Defb14.[20] This difference in charge state distribution can be attributed to the presence of three disulfide bridges in the wild-type Defb14, which limit the availability of protonation sites.

Under buffered conditions, the charge state distribution of each derivative is centered around $[M + 5H]^{5+}$, whereas under denaturing conditions there is an increase in the population of higher charge states with the most intense peak being $[M + 6H]^{6+}$. As anticipated, it appears that the presence of acid and organic solvent induces slightly more open conformations of the peptides in solution prior to ionization. Despite the different functional groups introduced at Cys^{V}, the mass spectra of the derivatives are remarkably similar to each other. Thus, by mass

TABLE 1: Mean Collision Cross Sections (Å^2) of the Derivatives Defb14-1X^V under Buffered and Denaturing Conditions[a]

	buffered conditions			denaturing conditions		
charge state	Defb14-1(Cy-1)^V	Defb14-1(Cy-2)^V	Defb14-1(Cy-3)^V	Defb14-1(Cy-1)^V	Defb14-1(Cy-2)^V	Defb14-1(Cy-3)^V
$[M + 3H]^{3+}$	586 ± 3	666 ± 28	586 ± 7	*b*	*b*	*b*
$[M + 4H]^{4+}$	761 ± 5	768 ± 10	777 ± 10	673 ± 13	676 ± 20	*b*
$[M + 5H]^{5+}$	987 ± 8	973 ± 17	969 ± 9	753 ± 13	758 ± 3	924 ± 32
$[M + 6H]^{6+}$	1033 ± 4	1040 ± 11	1056 ± 12	906 ± 22	909 ± 8	1021 ± 3
$[M + 7H]^{7+}$	1060 ± 18	1087 ± 18	1071 ± 8	1029 ± 15	1037 ± 3	1127 ± 12
$[M + 8H]^{8+}$	1110 ± 17	1126 ± 23	1136 ± 11	1089 ± 16	1123 ± 5	1235 ± 20
$[M + 9H]^{9+}$	1176 ± 19	1218 ± 18	1200 ± 12	1162 ± 7	1212 ± 4	1328 ± 31

[a] Errors are quoted as the standard error of the mean. [b] Not observed by IM-MS.

spectrometry alone we were unable to discern any structural differences between the active and inactive peptides. This prompted us to probe their conformations using ion mobility-mass spectrometry.

Ion Mobility-Mass Spectrometry. ***The Derivatives Adopt Similar Gas-Phase Geometries under Buffered Conditions.*** For all species studied by IM-MS under buffered conditions, we observe a single, relatively narrow arrival time distribution, implying that the gas-phase conformations adopted by each of these peptide ions are closely related in size. The collision cross-section of each ion increases with increasing charge (Table 1). Such an effect has been well-documented in other studies of proteins by ion mobility and can be attributed to expansion of the peptide structure to minimize Coulomb repulsion as an increasing number of protons are accepted.[11,23]

When ionized from 10 mM ammonium acetate, we measure similar collision cross sections for each of the derivatives at a given charge state. An exception is that the $[M + 3H]^{3+}$ ion of Defb14-1(Cy-2)^V is larger than the same charge state of Defb14-1(Cy-1)^V and Defb14-1(Cy-3)^V. In this case, it is possible that the "fixed" charges on the side-chains of Cy-1 and Cy-3 are involved in electrostatic interactions that constrict the structure of these ions at low charge states; at higher charge states, these proposed interactions may be less important as the peptide unfolds with increasing charge. In the main, however, it appears that the peptide derivatives in this study adopt similar gas-phase conformations to each other upon ionization from aqueous buffer. To survey a wider range of possible conformations and to examine the ease with which the peptides denature, we also ionized the peptides from an acidified solution of water/methanol.

Under Denaturing Conditions the Derivatives Exhibit Greater Gas-Phase Unfolding. As with the buffered conditions, we observe a single arrival time distribution for the species obtained from an acidified solution of water/methanol. However, the peaks are wider in the mobility spectra recorded under denaturing conditions; this is illustrated in Figure 4 for the $[M + 9H]^{9+}$ ion of Defb14-1(Cy-1)^V and is observed for all of the other species also. This observation implies that the peptides produced from acidified solution possess a greater range of peptide conformations in the gas-phase, though these different structures within a single charge state remain unresolvable in our IM-MS instrument. Separation of these various peptide conformations may be possible on instruments that possess longer drift tubes[24] or operate at higher buffer gas pressures.[25]

Again we observe an increase in collision cross-section with increasing charge (Table 1). When these cross sections are compared with those obtained from aqueous buffer, we note that there is a steeper increase in size between $[M + 5H]^{5+}$ and $[M + 9H]^{9+}$ for the species under denaturing conditions. Together with the increased peak width, this indicates the derivatives have greater conformational flexibility under these denaturing conditions. Although all peptide ions exhibit a greater range of sizes under denaturing conditions, the average cross sections of some peptide ions are smaller under denaturing conditions than under buffered conditions, especially at lower charge states. It is possible that this reflects the solution-phase change from unstructured peptide to helical peptide upon the addition of methanol.

It is clear that the different solution conditions have resulted in different geometries postionization. For example, the $[M + 4H]^{4+}$ to $[M + 6H]^{6+}$ ions of Defb14-1(Cy-1)^V and Defb14-1(Cy-2)^V are more compact under denaturing conditions than the equivalent ions produced from ammonium acetate. Meanwhile Defb14-1(Cy-3)^V is more extended at $z = 7-9$ under denaturing conditions. The ability to distinguish between protein ions obtained from different solutions has been reported previously; for example, Jarrold and co-workers measured different cross sections for ions of cytochrome *c* produced from buffered, acidified, and methanol-denatured solutions.[17] Here a similar approach shows how single chemical changes in the sequence of a given polypeptide can significantly alter its structural stability and by inference the ease by which it can unfold, as seen in the relative changes of collision cross section versus charge state. We now consider how the cross sections of these derivatives and other β-defensin peptides correlate to their chemotactic activities.

Chemotactic and Nonchemotactic Peptides Can Be Distinguished under Denaturing Conditions. In addition to the three derivatives of Defb14-1Cys^V discussed in this study, our panel of peptides (Figure 1) consists of Defb14, Defb14-1Cys^V, and Defb14−0Cys, whose cross sections have been reported previ-

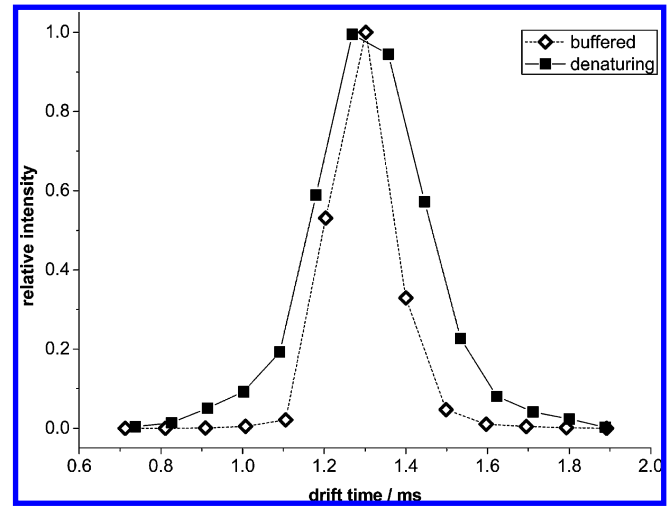

Figure 4. Drift time distributions for the $[M + 9]^{9+}$ ion of Defb14-1(Cy-1)^V at a drift voltage of 20 V under buffered and denaturing conditions. Drift times are scaled to 3.5 Torr and 37 °C to account for fluctuations in pressure and temperature between experiments.

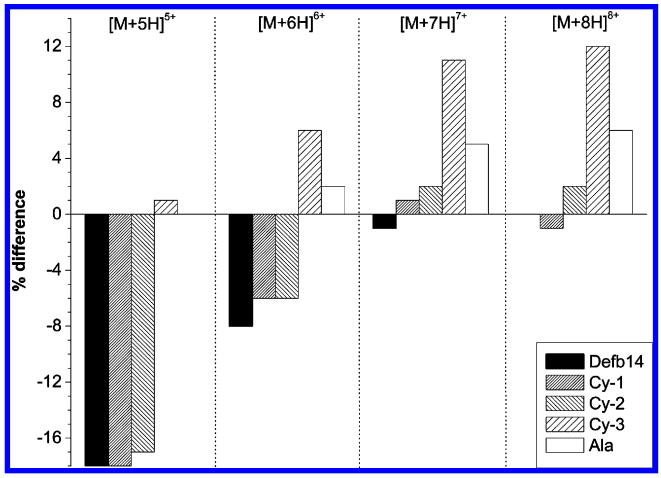

Figure 5. Comparison of collision cross sections of Defb14 and Defb14-1X^V derivatives versus unmodified Defb14-1Cys^V

ously (Supporting Information Table 1 and ref 20). Under denaturing conditions, the carboxymethylated and carboxamidomethylated derivatives have cross sections that are indistinguishable from unmodified Defb14-1Cys^V as $[M + 7H]^{7+}$ and $[M + 8H]^{8+}$ ions and similar to wild-type Defb14 for the charges states $z = 4-7$. Under these conditions the linear derivatives Defb14-1(Cy-1)^V and Defb14-1(Cy-2)^V exhibit remarkable gas-phase stability; they unfold similarly to wild-type Defb14, which is constrained by three intramolecular disulfide bonds. In contrast, the ethylamine derivative and Defb14-0Cys have significantly larger collision cross sections than Defb14-1Cys^V as $[M + 7H]^{7+}$ and $[M + 8H]^{8+}$ ions and greater than Defb14-1(Cy-1)^V, Defb14-1(Cy-2)^V and wild-type Defb14 across all of the observed charge states. We conclude from these observations that the small changes to the functionality at Cys^V have altered the conformational preferences of the peptides.

The peptides with chemotactic activity are significantly more compact at higher charge states than those that do not chemoattract, suggesting that the active peptides undergo less Coulomb-driven unfolding in the gas-phase. This is illustrated by considering the percentage change in the observed collision cross-section for the modified peptides versus unmodified Defb14-1Cys^V (Figure 5). The change in collision cross section due to the size of the substituent does not appear to be a factor here, since the smallest substituent (X = Ala) gives the second largest collision cross section for $z = 6$, 7, and 8. The Cy-3 and Cy-1 side-chains are of comparable size but the collision cross section for the $z = 8$ ion of Defb14-1(Cy-3)^V is 12% larger than that observed for the Defb14-1(Cy-1)^V. This may be due to Coulombic effects; if the amino group of Cy-3 is protonated, given its proximity to the basic residues in the C terminus of the peptide, it is likely that it will induce local unfolding due to electrostatic repulsion. The Cy-1 acidic group if deprotonated will interact favorably with the protonated basic groups thus tightening the conformation for this peptide.

In general, the active derivatives have similar cross sections to those of the wild-type Defb14, although Defb14-1Cys^V has a larger cross-section than the other active peptides at low charge states ($z = 5-6$). The reason for this is unclear but suggests that the unmodified cysteine peptide has a looser configuration than the other peptides with a smaller net number of charges.

The ability to discriminate between chemotactic and nonchemotactic peptides is dependent on the solution conditions prior to ionization. Under buffered conditions (Table 1 and Supporting Information Table 1), the peptides generally adopt similar geometries and we cannot make any distinction between the peptides of different activities. From a solution of acidified water/methanol, the peptides have a greater degree of conformational flexibility and can adopt different three-dimensional structures, as observed both by the widening of the arrival time distributions (Figure 4) and the relative change in the collision cross sections for the substituted peptides. Although this choice of solvent is clearly not representative of the environment of the receptor CCR6 in vivo, it does allow an in vacuo method to distinguish between ions from chemotactic and nonchemotactic derivatives of β-defensins.

Conclusions

The influence of synthetic single point mutations on the functional form that can be adopted by a 45 amino acid peptide has been highlighted by these findings. These results shed further light on the relationship between the structure and function of linear defensin analogs. Our previous work illustrated the importance of Cys^V to the chemotactic activity of HBD3 and Defb14. Here we have shown that it is likely that Cys^V of Defb14 does not interact directly with CCR6 but instead is important to the overall conformation of the peptide required to interact with the receptor. How these subtle chemical changes alter the ability of the peptide to interact favorably with CCR6 remains unresolved, however the structures of the isolated peptides are distinguishable by ion mobility-mass spectrometry under denaturing conditions. This technique may provide an interesting new approach to predict the chemotactic behavior of β-defensin derivatives and other chemotactic peptides. Ion mobility-mass spectrometry has been used to great effect in several previous studies to probe the unfolding of proteins[11] and, taking a similar approach, here we have shown how small changes to the sequence of a given peptide or protein can significantly affect its gas-phase unfolding behavior. Studies like this may also provide invaluable information to assist MD-based structure prediction, where ion mobility data could be used to provide coarse restraints to the folding of a given polypeptide.

Acknowledgment. This research was supported by the EPSRC Grants GR/S77639/01 and EP/C541561/1 and in particular via the award of an Advanced Research Fellowship to P.E.B. and a studentship to B.J.M. The Royal Society, the MRC, EaStCHEM, and the University of Edinburgh are also gratefully acknowledged for supporting this work. We also thank Bob Bateman and Waters Micromass Technologies as well as the British Mass Spectrometry Society.

Supporting Information Available: Collision cross sections of Defb14, Defb14-1Cys^V, and Defb14-0Cys under buffered and denaturing conditions. This material is available free of charge via the Internet at http://pubs.acs.org.

References and Notes

(1) Lehrer, R. I. *Nat. Rev. Microbiol.* **2004**, *2*, 727.
(2) Selsted, M. E.; Ouellette, A. J. *Nat. Immunol.* **2005**, *6*, 551.
(3) Pazgier, M.; Hoover, D. M.; Yang, D.; Lu, W.; Lubkowski, J. *Cell. Mol. Life Sci.* **2006**, *63*, 1294.
(4) Yang, D.; Chertov, O.; Bykovskaia, N.; Chen, Q.; Buffo, M. J.; Shogan, J.; Anderson, M.; Schroder, J. M.; Wang, J. M.; Howard, O. M. Z.; Oppenheim, J. J. *Science* **1999**, *286*, 525.
(5) Hancock, R. E. W.; Sahl, H. G. *Nat. Biotechnol.* **2006**, *24*, 1551.
(6) Wu, Z. B.; Hoover, D. M.; Yang, D.; Boulegue, C.; Santamaria, F.; Oppenheim, J. J.; Lubkowski, J.; Lu, W. Y. *Proc. Natl. Acad. Sci. U.S.A.* **2003**, *100*, 8880.
(7) Taylor, K.; Clarke, D. J.; McCullough, B.; Chin, W.; Seo, E.; Yang, D.; Oppenheim, J.; Uhrin, D.; Govan, J. R. W.; Campopiano, D. J.; MacMillan, D.; Barran, P.; Dorin, J. R. *J. Biol. Chem.* **2008**, *283*, 6631.

(8) Antcheva, N.; Morgera, F.; Creatti, L.; Vaccari, L.; Pag, U.; Pacor, S.; Shai, Y.; Sahl, H. G.; Tossi, A. *Biochem. J.* **2009**, *421*, 435.
(9) Rohrl, J.; Yang, D.; Oppenheim, J. J.; Hehlgans, T. *J. Biol. Chem.* **2008**, *283*, 5414.
(10) Pazgier, M.; Prahl, A.; Hoover, D. M.; Lubkowski, J. *J. Biol. Chem.* **2007**, *282*, 1819.
(11) Clemmer, D. E.; Jarrold, M. F. *J. Mass Spectrom.* **1997**, *32*, 577.
(12) Wyttenbach, T.; Bowers, M. T. *Annu. Rev. Phys. Chem.* **2007**, *58*, 511.
(13) Kanu, A. B.; Dwivedi, P.; Tam, M.; Matz, L.; Hill, H. H. *J. Mass Spectrom.* **2008**, *43*, 1.
(14) Wyttenbach, T.; Bowers, M. T. Gas-phase conformations: The ion mobility/ion chromatography method. In *Modern Mass Spectrometry*; Springer-Verlag: Berlin, 2003; Vol. 225. p 207.
(15) Wyttenbach, T.; vonHelden, G.; Bowers, M. T. *J. Am. Chem. Soc.* **1996**, *118*, 8355.
(16) Shelimov, K. B.; Clemmer, D. E.; Hudgins, R. R.; Jarrold, M. F. *J. Am. Chem. Soc.* **1997**, *119*, 2240.
(17) Hudgins, R. R.; Woenckhaus, J.; Jarrold, M. F. *Int. J. Mass Spectrom.* **1997**, *165*, 497.
(18) Schenauer, M. R.; Leary, J. A. *Int. J. Mass Spectrom.* **2009**, *287*, 70.
(19) McCullough, B. J.; Eastwood, H.; Clark, D. J.; Polfer, N. C.; Campopiano, D. J.; Dorin, J. A.; Maxwell, A.; Langley, R. J.; Govan, J. R. W.; Bernstein, S. L.; Bowers, M. T.; Barran, P. E. *Int. J. Mass Spectrom.* **2006**, *252*, 180.
(20) McCullough, B. J.; Kalapothakis, J.; Eastwood, H.; Kemper, P.; MacMillan, D.; Taylor, K.; Dorin, J.; Barran, P. E. *Anal. Chem.* **2008**, *80*, 6336.
(21) Nemethy, G.; Peer, W. J.; Scheraga, H. A. *Annu. Rev. Biophys. Bioeng.* **1981**, *10*, 459.
(22) Chowdhury, S. K.; Katta, V.; Chait, B. T. *J. Am. Chem. Soc.* **1990**, *112*, 9012.
(23) Valentine, S. J.; Counterman, A. E.; Clemmer, D. E. *J. Am. Soc. Mass Spectrom.* **1997**, *8*, 954.
(24) Kemper, P. R.; Dupuis, N. F.; Bowers, M. T. *Int. J. Mass Spectrom.* **2009**, *287*, 46.
(25) Pringle, S. D.; Giles, K.; Wildgoose, J. L.; Williams, J. P.; Slade, S. E.; Thalassinos, K.; Bateman, R. H.; Bowers, M. T.; Scrivens, J. H. *Int. J. Mass Spectrom.* **2007**, *261*, 1.

JP9111662